https://doi.org/10.5194/egusphere-2026-909
Preprint. Discussion started: 18 February 2026

Contrasting the gravity wave forcing between nudged and free-running models and reanalysis

Radek Zajíček[1], Zuzana Procházková[1], and Petr Šácha[1]
[1]Department of Atmospheric Physics, Faculty of Mathematics and Physics, Charles University, Prague, Czech Republic
Correspondence: Radek Zajíček (radek.zajicek@matfyz.cuni.cz) and Petr Šácha (petr.sacha@matfyz.cuni.cz)

Abstract. Internal gravity waves contribute to energy and momentum budgets across atmospheric layers. Hence, incorporating their dynamics through parameterization schemes is essential for Earth system models. However, any constraints on the parameterized gravity wave effects, especially on global spatial and climatological temporal scales, are practically non-existent. Here, we compare the recently published resolved gravity wave drag estimates and effects from the current generation high-resolution reanalysis with the climatology and dynamics in three different Earth system model simulations. The results show that except for differences in the mean value of gravity wave drag between the datasets, the parameterized drag in the models and the resolved drag in the reanalysis show very similar characteristics in terms of distribution and extremity. Despite this, we report pronounced differences in dynamical impacts of gravity waves between the reanalysis and the models in the lower stratosphere, where the parameterized gravity wave drag has a strong correlation with the Rossby wave forcing in the models. However, in ERA5 reanalysis we could not find any link between lower stratospheric resolved gravity and Rossby wave dynamics. This result indicates that the dynamical effects of gravity waves that we know from Earth system models can be different if gravity waves are resolved, which can have far-reaching implications for the gravity wave parameterization development and climate modeling and prompts further validation using alternative datasets in future work.

1 Introduction

Internal gravity waves (GWs) are a ubiquitous wave type occurring from the surface to the thermosphere in stably stratified atmospheric backgrounds (Nappo, 2012). In the troposphere, GWs are known to affect, for instance, the planetary boundary layer (Roy et al., 2021), cloud pattern and formation (Podglajen et al., 2018) or precipitation distribution (Cohen and Boos, 2017). Higher up, in the stratosphere and mesosphere, GWs are an important driver of global-scale circulations (Eichinger et al., 2020) and quasi-biennial oscillation period fluctuations (Kim, 2025). GW forcing is supposed to significantly influence also the dynamics of sudden stratospheric warmings (SSW), contributing to both changes in the meridional advection and zonal wind deceleration, with particularly strong effects at mesospheric levels during SSWs (Martínez-Andradas et al., 2025).

However, our understanding of large-scale GW impacts is mostly based on their parameterized effects in global climate models, because of fundamental limits on our ability to observe GWs on a global scale. In climate models, as a mesoscale phenomenon with typical scales smaller than the effective model resolution, GWs need to be parameterized based on numerous underlying simplifications (Plougonven et al., 2020) and including several free parameters that can be tuned specifically for

https://doi.org/10.5194/egusphere-2026-909
Preprint. Discussion started: 18 February 2026

each simulation by climate modeling centers. This tuning then strongly affects the resulting dynamics of the models in the stratosphere (Hájková and Šácha, 2024). Hence, our understanding of GW climate impacts can be model-dependent and can have an uncertain relation to the real atmosphere dynamics.

State-of-the-art climate models traditionally employ two GW parameterization schemes: a non-orographic GW parameterization for GWs sourced by convection, fronts, jets or spontaneous adjustment processes that is formulated and tuned to exert the strongest forcing in the tropics and in the upper stratosphere and mesosphere; and an orographic GW parameterization that accounts for the effects of subgrid-scale orography and produces strong forcing in the lower troposphere and throughout the extratropical stratosphere especially during the winter season. In many models (depending on the type and tuning of the particular scheme), the orographic GW parameterization provides the dominant forcing at the upper flank of the UTLS jet, the so-called valve layer.

Due to the columnar nature of the parameterization schemes, the horizontal distribution of parameterized orographic GW forcing strictly follows the terrestrial topography, resulting in sharply localized disturbances (so-called hotspots) to the model balanced meshes in the free atmosphere. Recent research has significantly advanced our understanding of the effects of orographic GW parameterizations on stratospheric dynamics and transport (Mehrdad et al., 2025; Hájková and Šácha, 2024; Šácha et al., 2021; Eichinger et al., 2020). In addition to the direct decelerating effect on the flow, it has been demonstrated that this parameterization also has a large indirect impact on the stratospheric circulation by affecting the propagation properties of resolved waves in the models. Depending on the position relative to the phase of the leading Rossby wave modes, the flow response to the parameterized GW drag (GWD) interferes constructively or destructively with the Rossby wave field. By modifying the refractive index in the valve layer, parameterized GWD effectively controls the Rossby wave propagation from the troposphere to the stratosphere, hence influencing the dynamics of the entire extratropical winter stratosphere.

Disentangling the effects of parameterized GWD in global climate models is a difficult task. First, the forcing is highly intermittent (Kuchař et al., 2020), and second, the dynamical interaction with the resolved wave field often leads to a compensating response of the circulation to anomalies in the parameterized GWD (Cohen et al., 2013, 2014). Therefore, the causality of the flow response cannot easily be disentangled and is being addressed by idealized model simulations with artificial drag enhancements (Šácha et al., 2016; Samtleben et al., 2020). Still, this approach is suboptimal because it does not reflect the other possible causal direction of the dynamical interaction, the impact of the background flow and the large-scale waves on parameterized GWs.

The goal of this study is to validate the dynamical interactions of parameterized GWD in the valve layer in global climate models using a quasi-observational dataset. For this, we analyse the dynamics associated with the resolved GW drag in ERA5 (Procházková et al., 2025b), as the best proxy for the real atmosphere GW forcing, and confront it with dynamical effects of parameterized GWs in nudged and transient climate model simulations. The paper is organized as follows. First, the reanalysis dataset and the method for GWD estimation are described followed by the description of the simulations and GW parameterizations in the models. The results section begins with an analysis of GWD and the Rossby wave drag climatologies and continues with an analysis of regional distribution and intermittency of GWD. Finally, we compare the dynamical interaction of GWs

https://doi.org/10.5194/egusphere-2026-909
Preprint. Discussion started: 18 February 2026

and Rossby waves between the reanalysis and the model simulations and conclude the paper by discussing the implications of the results presented.

2 Methodology

2.1 Data

The key ingredient for the study is the resolved GWD from ERA5 (Hersbach et al., 2017), which serves as a ground truth in our analysis. GWs are separated using the horizontal spherical harmonics filtering of hourly ERA5 data, based on model levels for the period 1979–2023. For the years 2000-2006, data based on ERA5.1, correcting the stratospheric temperature bias, were used (Simmons et al., 2020). The resulting GWD is due to waves with maximal horizontal wavelengths approximately 2000 km, separated from the mean flow by rhomboidal truncation. The full methodology of GWD computation is described in detail in (Procházková et al., 2025a).

The model part of the results is based on three climate model simulations, two nudged and one free running. We analyze the parameterized GWD from the Canadian Middle Atmosphere Model specified dynamics simulation (CMAM-sd; Scinocca et al., 2008; McLandress et al., 2013) for the 1979–2010 period with 71 levels in the vertical, extending up to 7×10^{-2} Pa (about 100 km) with variable vertical resolution. The horizontal resolution reflects the triangular spectral truncation of T47, corresponding to about 2.5° × 2.5°. For wavenumbers smaller than 21, Newtonian relaxation ("nudging") with a 24 h relaxation time-scale is applied toward the 6-hourly horizontal wind and temperature field from ERA-Interim up to 1 hPa (Dee et al., 2011). For further technical details see McLandress et al. (2014). Subgrid-scale orography (SSO) effects are parameterized using a three-component scheme comprising two freely propagating hydrostatic GW modes, low-level blocking and breaking processes and lee-vortex dynamics (Scinocca and McFarlane, 2000). Non-orographic GW effects are parameterized using the parameterization of Scinocca (2003), where a spectrum of hydrostatic GW modes in the absence of rotation is launched at 125 hPa. All the parameterized physics in the model is being performed on a 3.75° horizontal grid.

Further we analyze two simulations of the coupled chemistry-climate model The European Centre for Medium-Range Weather Forecasts Hamburg (ECHAM)/Modular Earth Submodel System (MESSy) Atmospheric Chemistry (EMAC) (Jöckel et al., 2016). The simulations have been produced and extensively described in the frame of the Earth System Chemistry Integrated Modelling (ESCiMo) (Jöckel et al., 2016). Both simulations have a horizontal resolution reflecting the triangular spectral truncation of T42 coresponding to a quadratic Gaussian grid of 2.8°×2.8° in latitude and longitude and 90 model levels in the vertical reaching up to 1 Pa (approximate altitude of 80 km). For comparison with ERA5 and CMAM-SD, we analyze a specific-dynamics simulation (RC1SD-base-10) with nudging of the prognostic variables (divergence, vorticity, temperature and surface pressure) towards ERA-Interim (Dee et al., 2011). In addition, we analyze a free running hindcast simulation from 1960 to 2010 (RC1-base-07a) driven with the observed sea-surface temperatures. Dynamical effects of SSO in EMAC are parameterized according to Lott and Miller (1997), which consists from two components, one for low-level blocking and the other for a single freely propagating hydrostatic orographic GW mode. Non-orographic GWs are parameterized with the Hines

https://doi.org/10.5194/egusphere-2026-909
Preprint. Discussion started: 18 February 2026

(1997) Doppler-spread parameterization scheme that launches a vertical-wavenumber spectrum at the 643 hPa level. For more details on the ESCiMo simulations, see Jöckel et al. (2016).

The two nudged simulations from different models have been selected for robustness of the results, as their circulation states are broadly similar to ERA5, while their parameterization schemes differ, and hence it is of interest to compare the resulting GWD. In the free-running simulation, the GWD effects can evolve freely, while the climatological background in the tropopshere remains similar to the other datasets due to the realistic sea surface temperatures.

Given the different lengths of the model simulations and ERA5, we restrict the analysis to the period 1979–2010, when all datasets are available. Although the main focus of the analysis is on the extratropical lower stratosphere during the boreal winter, where orographic GWD dominates, for consistency we use a sum of parameterized orographic and non-orographic drag from the models, as the GWD estimates from ERA5 cannot be generally separated into orographic and non-orographic GW contribution. This is also the case for regional drags above the main orographic hotspots of Northern Hemisphere (NH), where, however, one can assume even more firmly that orographic GW are dominant also in ERA5. Notably, when comparing ERA5 to the climate model simulations with the horizontal resolutions described above, the GW spectrum contributing to resolved GWD in ERA5 aligns well with the spectrum targeted by GW parameterizations in the models. This spectrum in ERA5 spans roughly 100–2000 km, while the models typically target around 200 km (see Hájková and Šácha (2024)).

For analyzing the effect of GWD on large-scale dynamics, Eliassen-Palm flux (EPF) and its divergence (EPFD) are being analyzed. For the models, EPFD has been provided by the modelling centers. For ERA5, EPFD from the Reanalysis Intercomparison Dataset (RID) (Martineau et al., 2018), computed on a regular 2.5°×2.5° grid, is used. This ensures consistency of the resolved wave field contributing to EPFD between the reanalysis and the models, and effectively filters out the contribution of gravity waves to EPFD in ERA5. In the focus region of our study, the extratropical stratosphere, EPFD is therefore dominated by Rossby waves.

2.2 Hotspot and composite construction

The hotspot-based part of the analysis is focused on 3 prominent GW activity regions in the Northern Hemisphere (NH) defined consistently with previous studies (e.g., Kuchař et al., 2020; Procházková et al., 2025a) - Himalayas (HI, 70–102.5°E and 20–40°N), West America (WA, 235–257.5°E and 27.5–52°N) and East Asia (EA, 110–145°E and 30–48°N). The representative parameterized GWD time series for each hotspot from the simulations were constructed by applying area-weighting (with the cosine of latitude as weights) and subsequently averaging the GWD values over all grid points within the defined region. The method of computing resolved GWD from ERA5 over the hotspots was described in Procházková et al. (2025a).

The GWD extreme states are analyzed using a composite analysis based on the detection of the strongest GWD events during boreal winter. To identify these events, we apply a peak-detection algorithm following the methodology of Kuchař et al. (2020). The algorithm defines peaks as local minima (the drag is negative) in the GWD time series whose amplitude exceeds 55% of the range between the seasonal maximum and minimum GWD values. In addition, only local minima separated from their nearest neighbors by at least 20 days are retained, ensuring that the detected events represent distinct and well-isolated episodes of enhanced GWD. The statistical significance of composite anomalies were constructed using a bootstrap method

https://doi.org/10.5194/egusphere-2026-909
Preprint. Discussion started: 18 February 2026

based on 10 000 samples and subsequently corrected for multiple testing using the Benjamini–Hochberg procedure (Benjamini and Hochberg, 1995).

3 Results

3.1 Zonal mean and hotspot climatology

Figure 1 shows the NH zonal mean zonal GWD climatological distribution for the boreal winter across all analyzed datasets. The zonal mean GWD distribution is very similar for all the datasets. There is a pronounced minimum at the upper flank of the subtropical jet for both resolved (ERA5, upper left plot in Fig. 1) and parameterized (rest of the plots in Fig. 1) GWD. Further aloft, the drag remains moderately strong along the edge of the polar vortex and from the middle stratosphere (around 20 hPa and aloft) it is growing in magnitude with height up to the top of our analysis. This is, however, seen only in the models, whereas in the reanalysis we only see a weak enhancement of the resolved GWD magnitude in the upper stratosphere up to 7 hPa. Here, the models show two distinct areas of strong GWD centered around 50°N and 65°N, but in ERA5 the drag is much weaker and the structure is less pronounced.

A closer inspection also reveals differences in the structure of the lower stratospheric drag minimum. The parameterized GWD is centered around 70 hPa for all models, whereas the resolved drag in ERA5 is shifted lower down closer to the tropopause. Another important difference between the resolved and parameterized drag is the narrower meridional distribution of strong GWD in the lower stratosphere in ERA5, centered directly above the center of the subtropical jet. This is not reflected in the models, where the region of strongest GWD is much broader meridionally. A likely cause is the oblique propagation and focusing of resolved GWs towards the center of the jet, as has been reported before (e.g., Kruse et al., 2022). Regarding magnitude, the drag in ERA5 in this region is again weaker than in the models - by around 50% than in CMAM-sd and both EMAC simulations have even stronger parameterized GWD in this region (and the specific dynamics version also in the upper stratosphere).

Because the goal of our paper is to compare the interaction of GWs and Rossby waves between the datasets, in Fig. 2 we also show the climatology of EPF and EPFD as a proxy for Rossby wave propagation and forcing analogously to Fig. 1. The boreal winter climatological distribution is again grossly similar between the models and the reanalysis, with the waves propagating upwards and equatorwards from the tropopause region in midlatitudes, where a narrow region of positive drag is located, and dissipating at the flanks of the jets. In particular, the CMAM-SD simulation captures the EPFD climatology from ERA5 remarkably well in terms of both distribution and magnitude of the drag. Both ESCiMo simulations do not produce the pronounced negative EPFD area above 70hPa along the edge of the polar vortex and the free running simulation also underestimates the drag enhancement, where the waves enter the polar night jet region. As a result, the polar jet is stronger in the free running EMAC simulation than in its specific dynamics run (see the countours in Fig. 1). The EPFD magnitude is similar between the datasets and note that it is about ten times the strength of GWD, which has a comparable magnitude only in the confined region above the center of the subtropical jet (Šácha et al., 2019).

https://doi.org/10.5194/egusphere-2026-909
Preprint. Discussion started: 18 February 2026

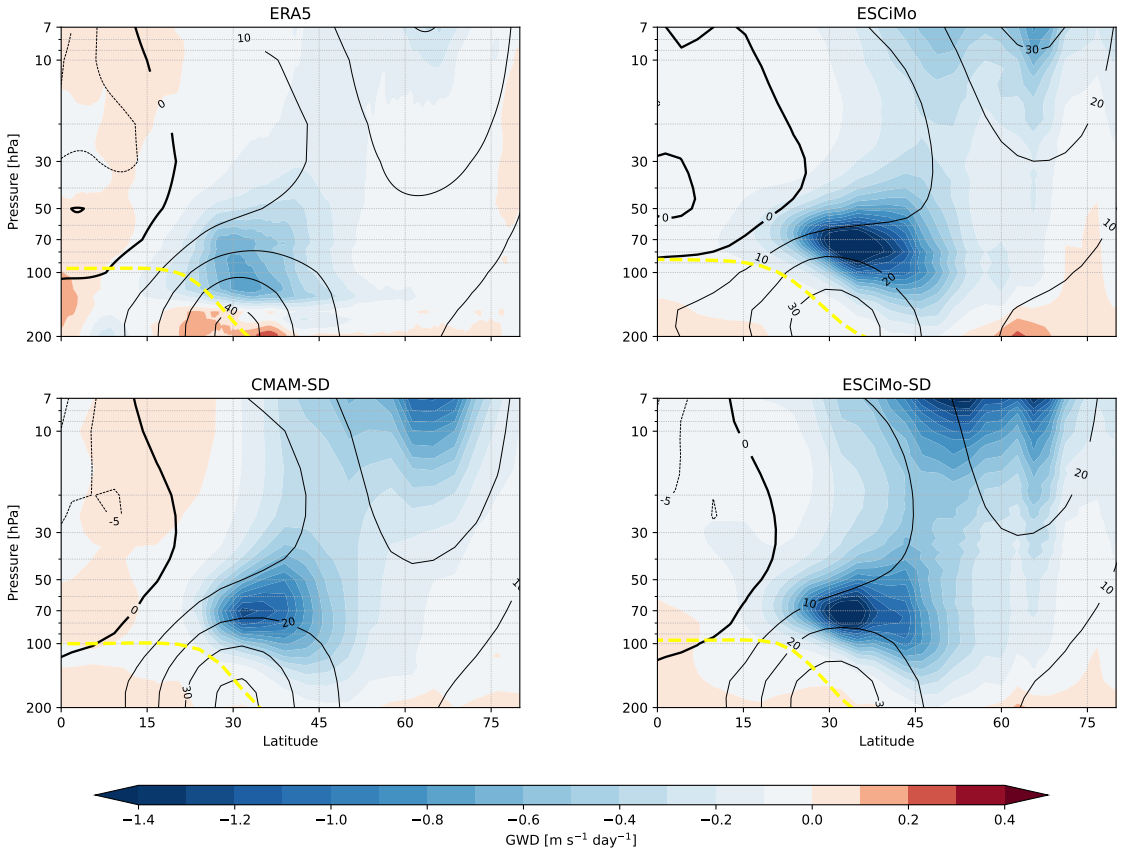

Figure 1. Zonal mean GWD climatology for boreal winter. Contours represent the zonal mean zonal wind in ms^{-1}. Yellow dashed line represents mean lapse-rate tropopause pressure.

3.2 Regional distribution and intermittency

It is well known that GWD is not distributed homogeneously in the zonal direction (Šácha et al., 2018). Hence, we take a closer look in Fig. 3 at the regional characteristics of the climatological drag above the three selected major NH hotspots (Himalayas, East Asia, West America) during boreal winter. For all hotspots, it can be seen that resolved GWD in ERA5 is weaker compared to parameterized GWD in the models. Over the Himalayas, the models consistently place strongest GWD near 70 hPa, where also resolved GWD in ERA5 has an extreme, but in ERA5 the drag peaks at around -1 m $\mathrm{s}^{-1}\mathrm{day}^{-1}$, whereas the models show good agreement in the peak amplitude (around -3.5 m $\mathrm{s}^{-1}\mathrm{day}^{-1}$).

In the East Asia hotspot, the lower stratospheric GWD minimum is almost absent in ERA5 and the resolved drag is distributed throughout the stratosphere. The lower stratospheric minimum is also less pronounced in the models, where GWD is

https://doi.org/10.5194/egusphere-2026-909
Preprint. Discussion started: 18 February 2026

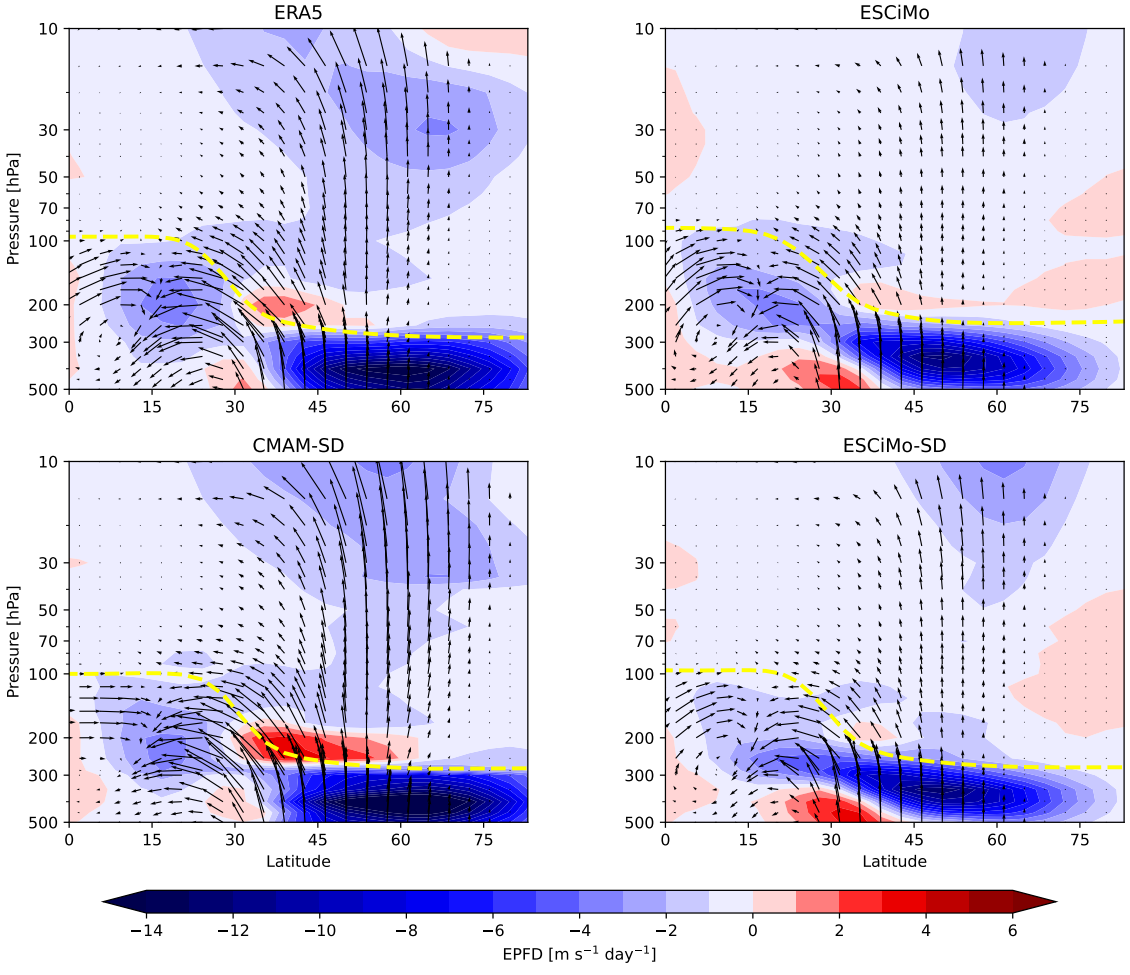

Figure 2. EPFD climatology for boreal winter. Arrows represents mean EPF whose components are scaled in a physically correct way in accordance with Jucker (2021). Yellow dashed line represents mean lapse-rate tropopause pressure.

more broadly spread between 50 and 70 hPa and exhibits a noticeably flatter vertical profile. In this hotspot, the models do not agree on the vertical position of the GWD extreme. Regarding the magnitude, if we take into account also the spread of GWD, which is especially for the models larger than for the other two hotspots, the parameterized drag values are closer to the resolved GWD in ERA5 in the East Asia hotspot.

For West America, the models agree on the height of the maximum (around 80 hPa), but differ substantially in its strength, with both ESCiMo simulations showing nearly twice the mean GWD at the peak compared to CMAM-SD. ERA5 GWD shows

https://doi.org/10.5194/egusphere-2026-909
Preprint. Discussion started: 18 February 2026

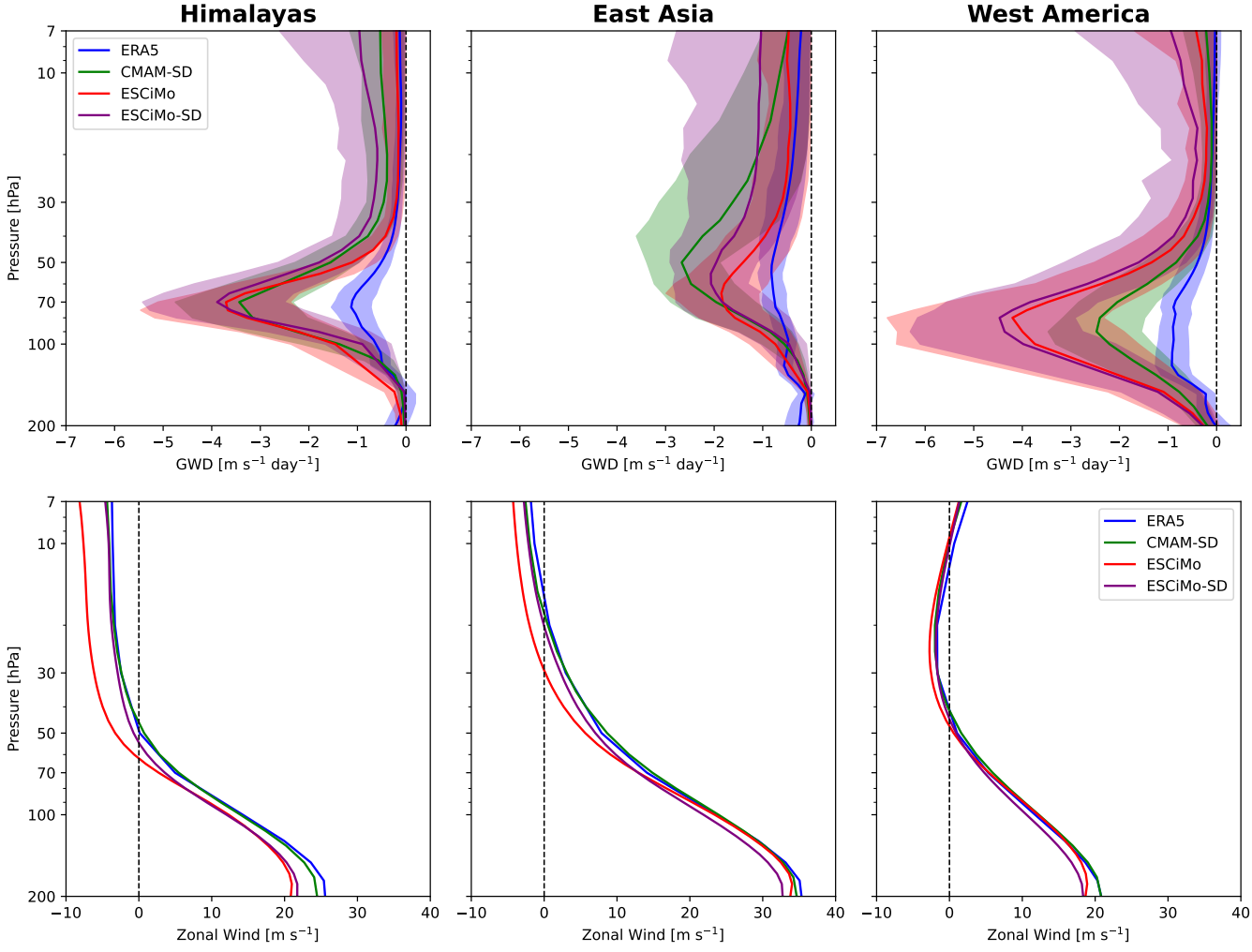

Figure 3. GWD (top row) and zonal wind (bottom row) hotspot-based climatology for boreal winter. Shading for GWD represents 10-90th percentile spread based on monthly mean values.

a flat peak between about 100 and 70 hPa with the mean values slightly below -1 m $s^{-1}day^{-1}$. The different vertical profiles between the East Asia hotspot and Himalayas and West America are likely due to the different climatological zonal wind profiles (bottom plots in Fig. 3). We see that the zonal winds in the stratosphere above the East Asia are stronger than above the other hotspots and the zero wind line (providing a critical layer for orographic GWs) is much higher here. Another factor that can play a role for resolved GWD in ERA5 is pressumably the higher portion of non-orographic GWs contributing to the

https://doi.org/10.5194/egusphere-2026-909
Preprint. Discussion started: 18 February 2026

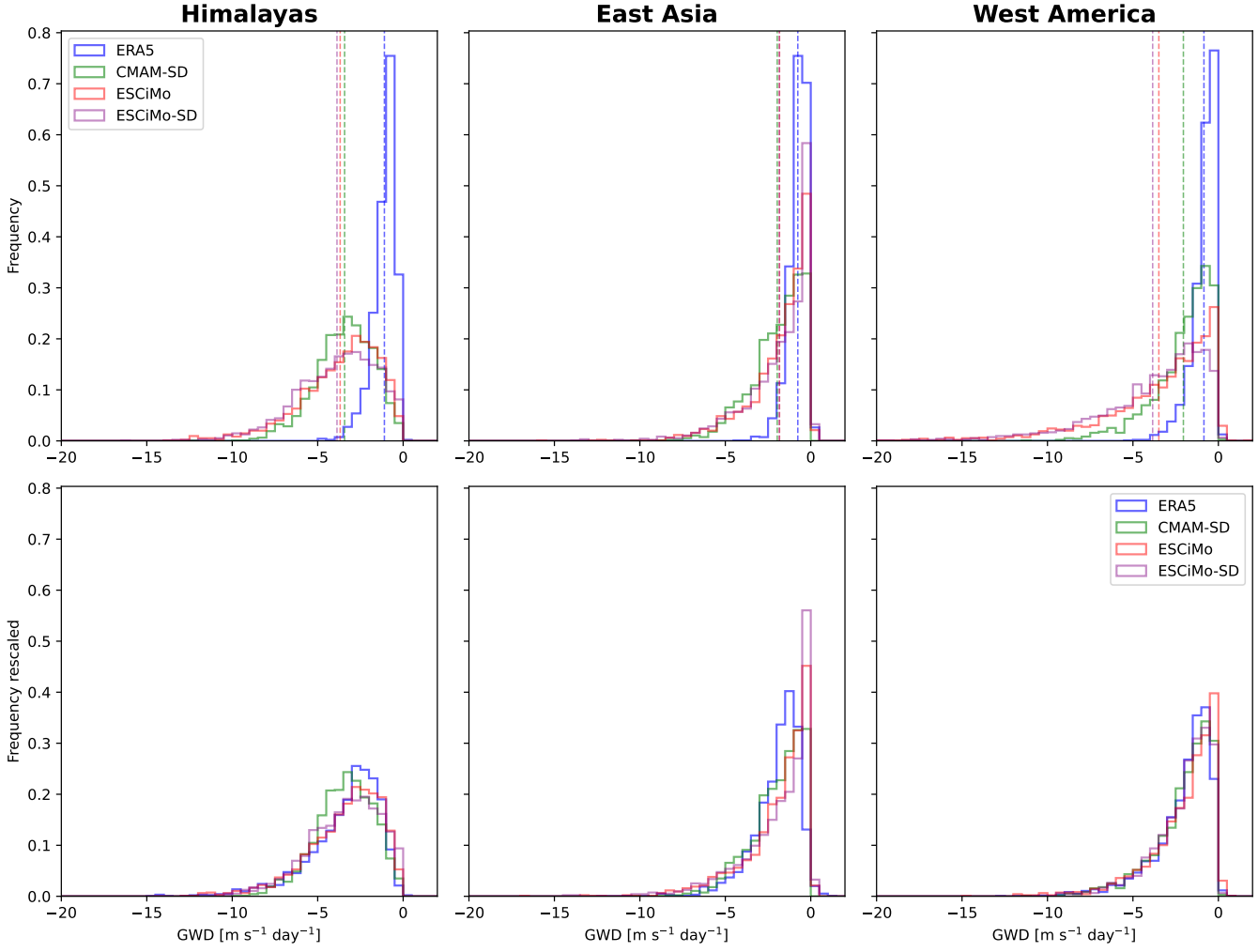

Figure 4. Histogram of daily GWD data at 70 hPa during boreal winter. Top row are original data with dashed line showing value of the mean for individual dataset, bottom row are histograms rescaled that all datasets have the same mean (corresponding to CMAM).

East Asia hotspot (Šácha et al., 2015) and possibly also oblique propagation of orographic GWs propagating from the sources in central Asia.

Surprisingly, much stronger GWD in the models than in ERA5 above 100 hPa is not clearly reflected in differences in the regionally averaged zonal wind. Especially above the West America and East Asia hotspots the model winds agree very well with ERA5 up to around 50 hPa. Only ESCiMo-SD clearly underestimates the maximal wind speed of the jet and generally the wind speed throughout the upper troposphere and above 50 hPa the underestimation is more pronounced in the transient

https://doi.org/10.5194/egusphere-2026-909
Preprint. Discussion started: 18 February 2026

Table 1. Number of detected peaks during boreal winter for individual hotspots and datasets. Value below represents threshold value for peak detection.

	Himalayas	East Asia	West America
ERA5	48 peaks 5.09 m s^{-1} day^{-1}	41 peaks 4.10 m s^{-1} day^{-1}	47 peaks 5.65 m s^{-1} day^{-1}
CMAM-SD	29 peaks 6.60 m s^{-1} day^{-1}	51 peaks 5.49 m s^{-1} day^{-1}	54 peaks 5.86 m s^{-1} day^{-1}
ESCiMo	57 peaks 7.40 m s^{-1} day^{-1}	33 peaks 8.28 m s^{-1} day^{-1}	34 peaks 12.55 m s^{-1} day^{-1}
ESCiMo-SD	30 peaks 8.80 m s^{-1} day^{-1}	47 peaks 7.37 m s^{-1} day^{-1}	52 peaks 10.77 m s^{-1} day^{-1}

simulation. Above Himalayas we see a pronounced underestimation of the climatological zonal wind speed for both ESCiMo simulations across the UTLS region, but CMAM-SD follows the ERA5 wind profile remarkably well.

We now shift our attention to analyzing the GWD spread in more detail and comparing the intermittency of GWD between the datasets. Figure 4 shows the probability density distributions of daily GWD magnitudes above the hotspots for all datasets at 70 hPa. The distribution of parameterized GWD is very similar across all model simulations. However, it differs substantially from ERA5 for all hotspots except East Asia. When we rescale the datasets to have the same mean GWD (shown by the dashed line in the top row), we see that the intermittency of the parameterized GWD for all simulations agrees remarkably well with that of the resolved GWD from ERA5. One difference to note is the East Asia hotspot and the peak of occurrence frequency shifted to stronger drags in ERA5 after rescaling. Here, the likely cause of this frequent weak drag regime can again be the oblique propagation of GWs from the Himalayas and Tibetian Plateau region, a feature completely missing in parameterizations.

To analyze the drag features at the long tails of the distribution in Fig. 4, we composite GWD above the hotspots with regard to the strong GWD events, detected as episodes with threshold exceeding 55% of the range between the seasonal maximum and minimum GWD values. The exact threshold values are variable for each dataset and hotspot as can be seen from Tab. 1 together with the number of events detected.

In Fig. 5 we see the best agreement among the models and ERA5 for the East Asia hotspot, where the strong GWD events have a similar duration and vertical structure across all datasets. For the Himalayas, the vertical structure is also similar, but in ERA5 the strong GWD event lasts for around 6 days, whereas in the models and particularly for the specific dynamics simulations the drag is significantly enhanced much earlier before and much longer after the peak. This is also partly true for the West America hotspot, but here the parameterizations in the models do a good job in capturing the nontrivial vertical structure of the event in ERA5, which suggests that the strong GWD events diagnosed at 70 hPa are not only confined to the lower stratosphere, but are connected with significant drag enhancements across the stratosphere.

https://doi.org/10.5194/egusphere-2026-909
Preprint. Discussion started: 18 February 2026

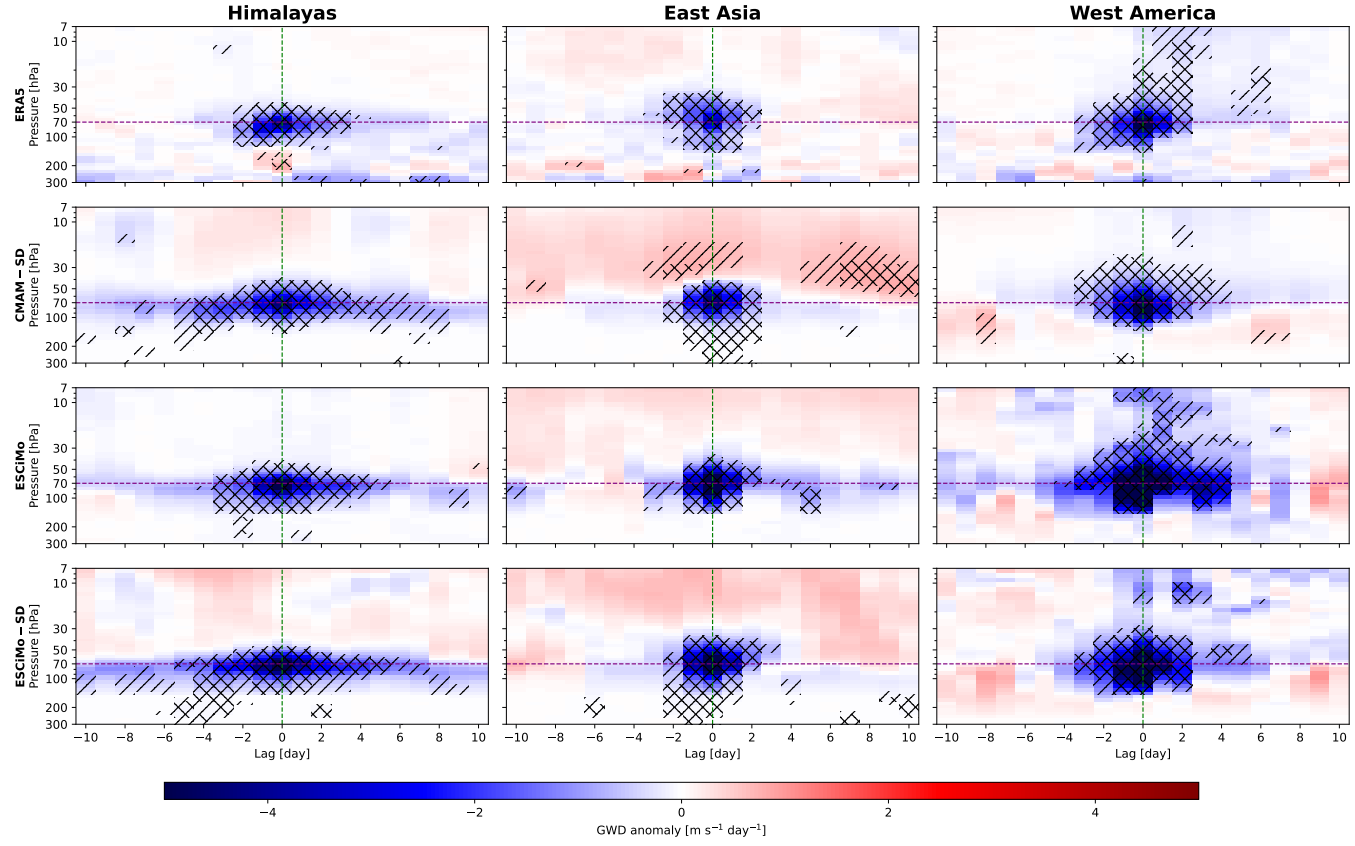

Figure 5. Lagged evolution of composite anomalies of GWD within the selected hotspot during strongest boreal peaks for individual hotspots (columns) and datasets (rows). Values for ERA5 (first row) are multiplied by 2 for easier interpretation. Purple lines represent the composite level of 70 hPa. Hatching \\ and // represents p-values less than 0.05 and 0.01.

3.3 GWD-EPFD interaction

After analyzing the drag characteristics, we now focus on the interaction between GWD and Rossby wave forcing quantified by EPFD, which is the ultimate goal of this study. Figure 6 shows the point-wise correlations of daily zonal mean GWD and EPFD in the boreal winter NH stratosphere. We focus particularly on the valve layer (region in the extratropical lower stratosphere), where the GWD minimum has been shown before to modify the Rossby wave propagation (Šácha et al., 2021; Sigmond et al., 2023; Hájková and Šácha, 2024), leading to a compensation response in the models between the parameterized and resolved drag (Cohen et al., 2013). This behavior is clearly visible in the plots for the specific dynamics simulations as a significant anti-correlation slightly southward from the parameterized drag minimum (GWD is depicted with contours). For the transient simulation the significant anti-correlation extends across the whole meridional span of the GWD minimum. However, this statistical relationship documenting the leading dynamical effect of parameterized GWD in the models is only weakly

https://doi.org/10.5194/egusphere-2026-909
Preprint. Discussion started: 18 February 2026

supported by ERA5. The resolved GWD is only weakly correlated with EPFD and the area of significant correlation is much smaller than in the models.

In Fig. 7 we take a closer look at the region of the significant correlations and strongest GWD (50-70 hPa; 20-30°N) and show a two-dimensional histogram of daily GWD and EPFD values within this region. The compensation mechanism between parameterized GWD and EPFD is again very clearly pronounced for the models. The relationship is very similar for both specific dynamics simulations. For the transient simulation the range of drag values is more broadly distributed, but the signal is still clearly discernible. In contrast to this, there is almost no statistical relationship between the resolved GWD and EPFD in ERA5, which raises the question of whether the extratropical lower-stratospheric dynamics inferred from coarse-resolution models remain valid when gravity waves are at least partially resolved. Implications of this finding and remaining uncertainty of our analysis are discussed in the next section.

4 Conclusions

Comparing recently published resolved GWD estimates for ERA5 by Procházková et al. (2025a) with parameterized GWD from climate model simulations, we have shown that there is good agreement in climatological features of the parameterized drag from models in the NH winter with the "quasi-observational" estimates from the reanalysis, both in a zonal mean and regionally. We have identified only minor differences in the structure, however, also substantial differences in the magnitude of GWD in the lower stratosphere. When accounting for the differences in the mean drag value, we have further shown that the probability distribution of the GWD magnitude is almost exactly similar between the datasets. In addition, the composites of the strongest GWD events above regional hotspots in the lower stratosphere reveal an excellent agreement in characteristics of the extreme drag episodes.

That said, despite the similarities between the datasets our results show that the dominant dynamical effect of parameterized GWD in the models - the alteration of the Rossby wave field, which is extensively documented in the literature and also in our results, is not reflected in ERA5. For resolved GWD from ERA5 we have found a very weak to non-existent relationship with the Rossby waves in the valve layer. This finding questions not only our understanding of GW climate impacts, which has so far been based on their parameterized effects in the climate models, but also the realism of stratospheric dynamics in the models.

However, before making a definitive statement about the validity of the dynamical effects of GW parameterizations, we must first discuss how good a proxy the GWD estimates from ERA5 presented here are for real atmospheric dynamics. Recently, it has been shown that although ERA5 captures well the position and timing of directly observed GWs, it significantly underestimates their amplitudes and corresponding momentum fluxes (Gupta et al., 2024a; Lear et al., 2024), and hence also GWD. Further, it has to be noted that ERA5 also uses GW parameterizations to supplement the effects of the GW spectrum it cannot resolve, but these data are available only via a sum of all physics tendencies, which is not suitable for the goals of our paper. This is because the wind tendency from parameterized physics in the stratosphere also includes the contribution from the turbulence parameterization that is triggered by instabilities of the resolved GWs, which are captured in our resolved GWD

https://doi.org/10.5194/egusphere-2026-909
Preprint. Discussion started: 18 February 2026

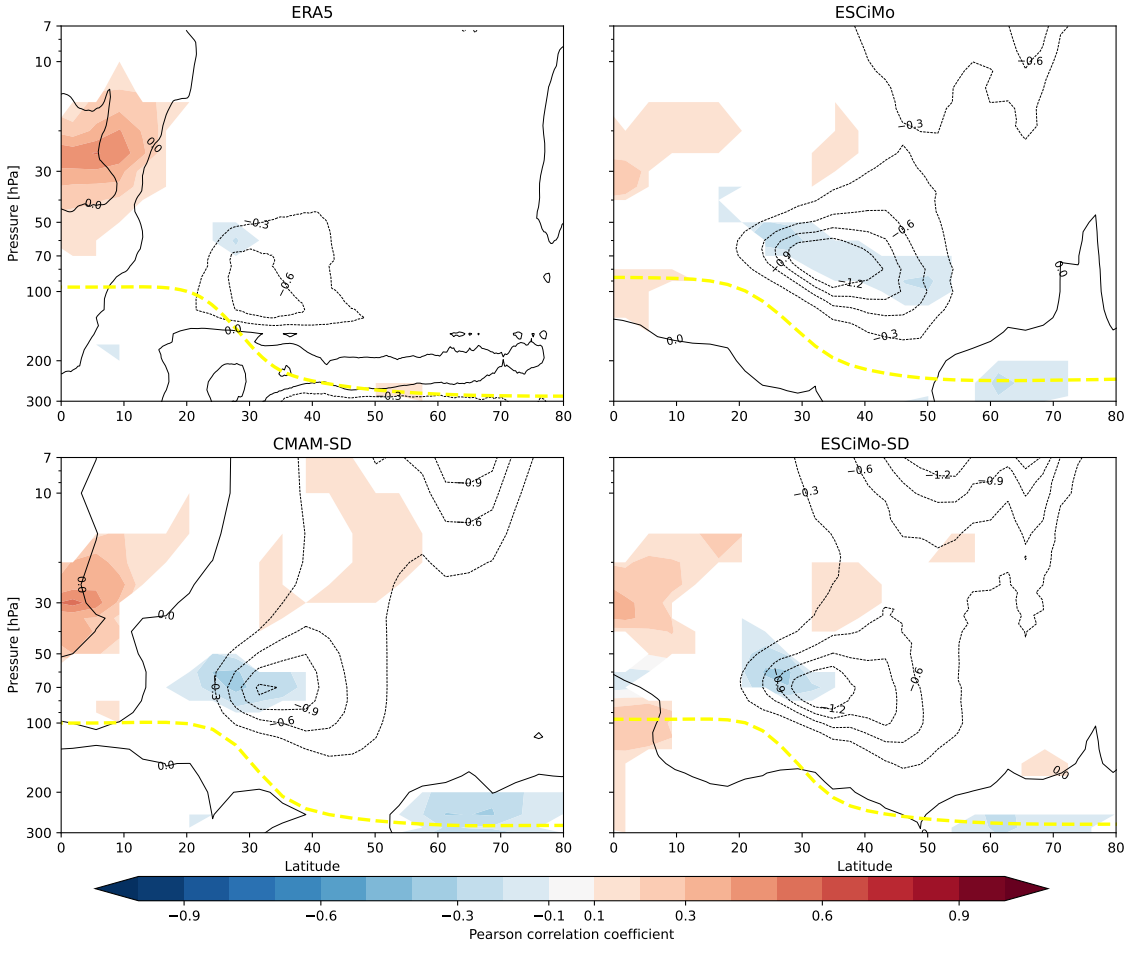

Figure 6. Pearson correlation between GWD and EPFD during boreal winter based on daily means. Contours represent zonal mean GWD in m s^{-1} day^{-1} Only regions with a statistical significance of correlations based on exceeding the 95% confidence level are plotted. Yellow dashed line represents mean lapse-rate tropopause pressure.

estimates and would result in possible double-counting of the drag. Other than this, analysis increments also enter the momentum budget and they are not available for the analysis as well. Preliminary results from closing the zonal mean momentum budget in ERA5 similarly to older reanalyses in the frame of the TEM equations (Fujiwara et al., 2024) indicate that the zonal mean resolved GWD presented here represents more than a half of the residual (not explainable by planetary and synoptic scale waves) drag in ERA5 in the valve layer (personal communication with Prof. Masatomo Fujiwara). Hence, we can expect that the real GW contribution (resolved, parameterized and the analysis increment together) to the drag in the valve layer will be closer to the magnitude of parameterized GWD in the models. This is also supported by the similarity of the mean wind between ERA5 and the simulations.

https://doi.org/10.5194/egusphere-2026-909
Preprint. Discussion started: 18 February 2026

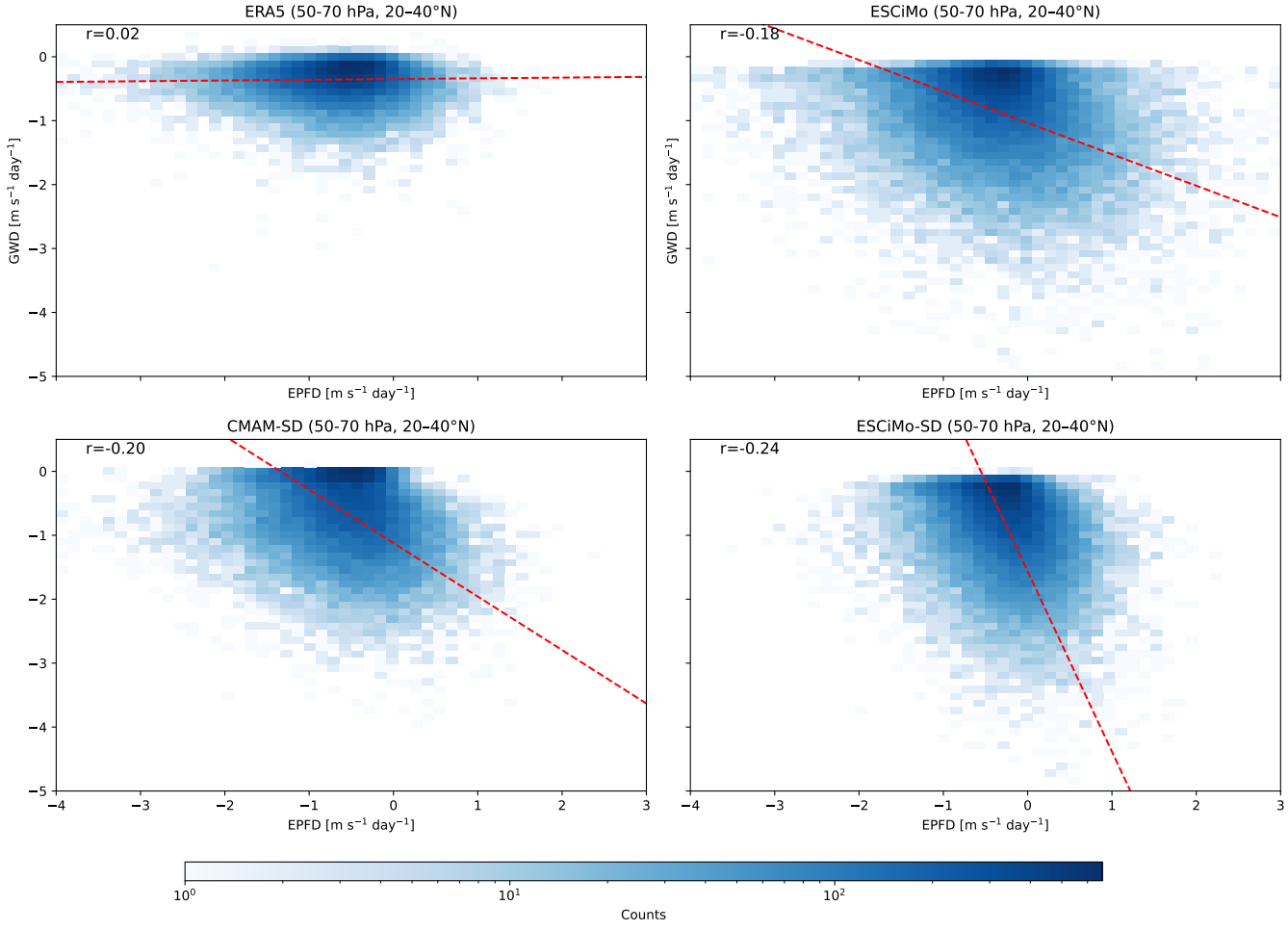

Figure 7. Two-dimensional histogram of GWD and EPFD within 50-70 hPa and 20-30°N region based on daily mean values during boreal winter. The red line shows the Deming regression line between GWD and EPFD. The Pearson correlation coefficient (r) is also indicated.

Can the smaller GWD magnitude in ERA5 be the cause of the missing signal of the compensation mechanism between the Rossby wave induced drag and GWD in the valve layer? We are skeptical about this, because the intermodel correlations presented by Hájková and Šácha (2024) (see their Figs. 4 and 6) do not suggest the existence of a threshold GWD value, at which the mechanism should start acting. Their results suggest that the relation between GWD and EPFD (and the refractive index in the valve layer) is linear and also holds for models with much smaller parameterized GWD magnitudes than the mean resolved GWD value in ERA5 in the lower stratosphere. Hence, we find it unlikely that a difference of around 1 m $s^{-1}day^{-1}$ in GWD magnitude will enhance or completely change the interaction between GWD and Rossby waves in the lower stratosphere.

Arguably, a more likely reason for the difference in the dynamical interaction can be the differences in how the resolved and parameterized GWD act on the flow. Whereas the resolved GW instability and consequent dissipation affect only a part

https://doi.org/10.5194/egusphere-2026-909
Preprint. Discussion started: 18 February 2026

of the GW field with a particular phase, parameterized GWD is communicated to the dynamical core of the models abruptly as instantaneous and homogeneous blocks of grid-scale tendencies. Also, due to the columnar approach utilized in GW parameterization schemes of current generation climate models, particularly the drag from orographic GW parameterizations strictly copies the distribution of continents and hence the planetary wave structure and phase of stationary Rossby waves that dominate the winter stratosphere dynamics. This way, the parameterized GWD can interact more efficiently with the planetary waves than the resolved GWD in ERA5 that is distributed more uniformly due to lateral propagation (Gupta et al., 2024b).

The strong dynamical effect of GW parameterizations on the Rossby wave field through the refractive index in the valve layer, which we see in current climate models, also influences phenomena directly linked with the circulation in the troposphere, such as SSWs and their frequency (Sigmond et al., 2023). It is therefore important to resolve the question, how realistic are the parameterized GWD effects, for informing the GW parameterization development. Most of the efforts so far have focused on constraining the magnitude of GW momentum fluxes (and hence the magnitude of the drag) from observations and did not consider how the resulting drag interacts with the resolved fields. Hence, for future work we see it vital to constrain the GWD dynamical effects from ensembles of high or ultra high resolution free running simulations of sufficiently long duration.

Data availability. Full computed ERA5 GWD time series can be made available upon request due to their size, a smaller version with reduced vertical grid can be downloaded at 10.5281/zenodo.15473685 (Procházková et al., 2025b). EPFD diagnostics for ERA5 were obtained from Reanalysis Intercomparison Dataset (RID) from https://www.jamstec.go.jp/ridinfo/ (last access: 13 February 2026)(Martineau et al., 2018). CMAM data were obtained from http://climate-modelling.canada.ca/climatemodeldata/cmam/output/CMAM/CMAM30-SD/index.shtml (last access: 13 February 2026). ESCiMo simulations are stored at German Climate Computing Centre (DKRZ) and can be made available upon request.

Author contributions. RZ: investigation, methodology, visualization. ZP: data curation, methodology. PŠ: conceptualization, interpretation of results, supervision. All authors contributed to writing.

Competing interests. The authors declare that they have no conflict of interest.

Acknowledgements. The authors want to thank Roland Eichinger for helping with the model data acquisition and acknowledge the utilization of the RID, which was produced by the Japan Agency for Marine-Earth Science and Technology, is used in this study (https://www.jamstec.go.jp/ridinfo/). We acknowledge the German Climate Computing Centre (DKRZ) supported from the Bundesministerium für Bildung und Forschung (BMBF) for providing the HPC and data archiving resources as well as the consortial project ESCiMo (Earth System Chemistry integrated Modelling) within which the EMAC simulations have been performed. ZP, PS and RZ were supported by the JUNIOR STAR project "Un-

https://doi.org/10.5194/egusphere-2026-909
Preprint. Discussion started: 18 February 2026

ravelling climate impacts of atmospheric internal gravity waves" under 23-04921M and ZP and PS also partly by GAČR project "Unravelling Subgrid-Scale Orography Effects on Composition in the Free Atmosphere (SCOPE)" under 25-17683S.

https://doi.org/10.5194/egusphere-2026-909
Preprint. Discussion started: 18 February 2026

References

Benjamini, Y. and Hochberg, Y.: Controlling the False Discovery Rate: A Practical and Powerful Approach to Multiple Testing, Journal of the Royal Statistical Society: Series B (Methodological), 57, 289–300, https://doi.org/https://doi.org/10.1111/j.2517-6161.1995.tb02031.x, 1995.

Cohen, N. Y. and Boos, W. R.: The influence of orographic Rossby and gravity waves on rainfall, Quarterly Journal of the Royal Meteorological Society, 143, 845–851, https://doi.org/https://doi.org/10.1002/qj.2969, 2017.

Cohen, N. Y., Gerber, E. P., and Bühler, O.: Compensation between Resolved and Unresolved Wave Driving in the Stratosphere: Implications for Downward Control, Journal of the Atmospheric Sciences, 70, 3780 – 3798, https://doi.org/10.1175/JAS-D-12-0346.1, 2013.

Cohen, N. Y., Gerber, E. P., and Bühler, O.: What Drives the Brewer–Dobson Circulation?, Journal of the Atmospheric Sciences, 71, 3837 – 3855, https://doi.org/10.1175/JAS-D-14-0021.1, 2014.

Dee, D. P., Uppala, S., Simmons, A. J., Berrisford, P., Poli, P., Kobayashi, S., Andrae, U., Balmaseda, M., Balsamo, G., Bauer, d. P., et al.: The ERA-Interim reanalysis: Configuration and performance of the data assimilation system, Quarterly Journal of the royal meteorological society, 137, 553–597, https://doi.org/10.1002/qj.828, 2011.

Eichinger, R., Garny, H., Šácha, P., Danker, J., Dietmüller, S., and Oberländer-Hayn, S.: Effects of missing gravity waves on stratospheric dynamics; part 1: climatology, Climate Dynamics, 54, 3165–3183, https://doi.org/10.1007/s00382-020-05166-w, 2020.

Fujiwara, M., Martineau, P., Wright, J. S., Abalos, M., Šácha, P., Kawatani, Y., Davis, S. M., Birner, T., and Monge-Sanz, B. M.: Climatology of the terms and variables of transformed Eulerian-mean (TEM) equations from multiple reanalyses: MERRA-2, JRA-55, ERA-Interim, and CFSR, Atmospheric Chemistry and Physics, 24, 7873–7898, https://doi.org/10.5194/acp-24-7873-2024, 2024.

Gupta, A., Reichert, R., Dörnbrack, A., Garny, H., Eichinger, R., Polichtchouk, I., Kaifler, B., and Birner, T.: Estimates of Southern Hemispheric Gravity Wave Momentum Fluxes across Observations, Reanalyses, and Kilometer-Scale Numerical Weather Prediction Model, Journal of the Atmospheric Sciences, 81, 583–604, https://doi.org/10.1175/JAS-D-23-0095.1, 2024a.

Gupta, A., Sheshadri, A., Alexander, M. J., and Birner, T.: Insights on lateral gravity wave propagation in the extratropical stratosphere from 44 years of ERA5 data, Geophysical Research Letters, 51, e2024GL108 541, https://doi.org/10.1029/2024GL108541, 2024b.

Hájková, D. and Šácha, P.: Parameterized orographic gravity wave drag and dynamical effects in CMIP6 models, Climate Dynamics, 62, 2259–2284, https://doi.org/10.1007/s00382-023-07021-0, 2024.

Hersbach, H., Bell, B., Berrisford, P., Hirahara, S., Horányi, A., Muñoz-Sabater, J., Nicolas, J., Peubey, C., Radu, R., Schepers, D., et al.: Complete ERA5 from 1940: Fifth generation of ECMWF atmospheric reanalyses of the global climate, Copernicus Climate Change Service (C3S) Data Store (CDS), 10, data distribution by the German Climate Computing Center (DKRZ), 2017.

Hines, C. O.: Doppler-spread parameterization of gravity-wave momentum deposition in the middle atmosphere. Part 1: Basic formulation, Journal of Atmospheric and Solar-Terrestrial Physics, 59, 371–386, https://doi.org/10.1016/S1364-6826(96)00079-X, 1997.

Jöckel, P., Tost, H., Pozzer, A., Kunze, M., Kirner, O., Brenninkmeijer, C. A. M., Brinkop, S., Cai, D. S., Dyroff, C., Eckstein, J., Frank, F., Garny, H., Gottschaldt, K.-D., Graf, P., Grewe, V., Kerkweg, A., Kern, B., Matthes, S., Mertens, M., Meul, S., Neumaier, M., Nützel, M., Oberländer-Hayn, S., Ruhnke, R., Runde, T., Sander, R., Scharffe, D., and Zahn, A.: Earth System Chemistry integrated Modelling (ESCiMo) with the Modular Earth Submodel System (MESSy) version 2.51, Geoscientific Model Development, 9, 1153–1200, https://doi.org/10.5194/gmd-9-1153-2016, 2016.

Jucker, M.: Scaling of Eliassen-Palm flux vectors, Atmospheric Science Letters, 22, e1020, https://doi.org/https://doi.org/10.1002/asl.1020, 2021.

https://doi.org/10.5194/egusphere-2026-909
Preprint. Discussion started: 18 February 2026

Kim, Y.-H.: Explaining the period fluctuation of the quasi-biennial oscillation, Atmospheric Chemistry and Physics, 25, 5647–5664, https://doi.org/10.5194/acp-25-5647-2025, 2025.

Kruse, C. G., Alexander, M. J., Hoffmann, L., van Niekerk, A., Polichtchouk, I., Bacmeister, J. T., Holt, L., Plougonven, R., Šácha, P., Wright, C., et al.: Observed and modeled mountain waves from the surface to the mesosphere near the Drake Passage, Journal of the atmospheric sciences, 79, 909–932, https://doi.org/10.1175/JAS-D-21-0252.1, 2022.

Kuchař, A., Šácha, P., Eichinger, R., Jacobi, C., Pišoft, P., and Rieder, H. E.: On the intermittency of orographic gravity wave hotspots and its importance for middle atmosphere dynamics, Weather and Climate Dynamics, 1, 481–495, https://doi.org/10.5194/wcd-1-481-2020, 2020.

Lear, E. J., Wright, C. J., Hindley, N. P., Polichtchouk, I., and Hoffmann, L.: Comparing Gravity Waves in a Kilometer-Scale Run of the IFS to AIRS Satellite Observations and ERA5, Journal of Geophysical Research: Atmospheres, 129, e2023JD040 097, https://doi.org/10.1029/2023JD040097, 2024.

Lott, F. and Miller, M. J.: A new subgrid-scale orographic drag parametrization: Its formulation and testing, Quarterly Journal of the Royal Meteorological Society, 123, 101–127, https://doi.org/10.1002/qj.49712353704, 1997.

Martineau, P., Wright, J. S., Zhu, N., and Fujiwara, M.: Zonal-mean data set of global atmospheric reanalyses on pressure levels, Earth System Science Data, 10, 1925–1941, https://doi.org/10.5194/essd-10-1925-2018, 2018.

Martínez-Andradas, V., de la Cámara, A., Zurita-Gotor, P., Lott, F., and Serva, F.: Quantifying the spread in sudden stratospheric warming wave forcing in CMIP6, Weather and Climate Dynamics, 6, 329–343, https://doi.org/10.5194/wcd-6-329-2025, 2025.

McLandress, C., Scinocca, J. F., Shepherd, T. G., Reader, M. C., and Manney, G. L.: Dynamical Control of the Mesosphere by Orographic and Nonorographic Gravity Wave Drag during the Extended Northern Winters of 2006 and 2009, Journal of the Atmospheric Sciences, 70, 2152 – 2169, https://doi.org/10.1175/JAS-D-12-0297.1, 2013.

McLandress, C., Plummer, D., and Shepherd, T.: A simple procedure for removing temporal discontinuities in ERA-Interim upper stratospheric temperatures for use in nudged chemistry-climate model simulations, Atmospheric Chemistry and Physics, 14, 1547–1555, 2014.

Mehrdad, S., Marjani, S., Handorf, D., and Jacobi, C.: Non-zonal gravity wave forcing of the Northern Hemisphere winter circulation and effects on middle atmosphere dynamics, Weather and Climate Dynamics, 6, 1491–1514, https://doi.org/10.5194/wcd-6-1491-2025, 2025.

Nappo, C. J.: An introduction to atmospheric gravity waves, vol. 102, Academic press, 2012.

Plougonven, R., de la Cámara, A., Hertzog, A., and Lott, F.: How does knowledge of atmospheric gravity waves guide their parameterizations?, Quarterly Journal of the Royal Meteorological Society, 146, 1529–1543, https://doi.org/10.1002/qj.3732, 2020.

Podglajen, A., Plougonven, R., Hertzog, A., and Jensen, E.: Impact of gravity waves on the motion and distribution of atmospheric ice particles, Atmospheric Chemistry and Physics, 18, 10 799–10 823, https://doi.org/10.5194/acp-18-10799-2018, 2018.

Procházková, Z., Zajíček, R., and Šácha, P.: Climatology, long-term variability and trend of resolved gravity wave drag in the stratosphere revealed by ERA5, Weather and Climate Dynamics, 6, 927–947, https://doi.org/10.5194/wcd-6-927-2025, 2025a.

Procházková, Z., Zajíček, R., and Šácha, P.: ERA5 gravity wave fluxes and drag on subdomains and in zonal mean [Dataset], https://doi.org/https://doi.org/10.5281/zenodo.15473686, Zenodo, 2025b.

Roy, S., Sentchev, A., Schmitt, F., Augustin, P., and Fourmentin, M.: Impact of the Nocturnal Low-Level Jet and Orographic Waves on Turbulent Motions and Energy Fluxes in the Lower Atmospheric Boundary Layer, Boundary-Layer Meteorology, 180, https://doi.org/10.1007/s10546-021-00629-x, 2021.

Šácha, P., Kuchař, A., and Pišoft, P.: Enhanced internal gravity wave activity and breaking over the northeastern Pacific–eastern Asian region, Atmospheric Chemistry and Physics, 15, 13 097–13 112, https://doi.org/10.5194/acp-15-13097-2015, 2015.

https://doi.org/10.5194/egusphere-2026-909
Preprint. Discussion started: 18 February 2026

Šácha, P., Lilienthal, F., Jacobi, C., and Pišoft, P.: Influence of the spatial distribution of gravity wave activity on the middle atmospheric dynamics, Atmospheric Chemistry and Physics, 16, 15 755–15 775, https://doi.org/10.5194/acp-16-15755-2016, 2016.

Šácha, P., Miksovsky, J., and Pisoft, P.: Interannual variability in the gravity wave drag–vertical coupling and possible climate links, Earth System Dynamics, 9, 647–661, https://doi.org/10.5194/esd-9-647-2018, 2018.

Šácha, P., Eichinger, R., Garny, H., Pišoft, P., Dietmüller, S., de la Torre, L., Plummer, D. A., Jöckel, P., Morgenstern, O., Zeng, G., et al.: Extratropical age of air trends and causative factors in climate projection simulations, Atmospheric Chemistry and Physics, 19, 7627–7647, https://doi.org/10.5194/acp-2018-1310, 2019.

Šácha, P., Kuchař, A., Eichinger, R., Pišoft, P., Jacobi, C., and Rieder, H. E.: Diverse Dynamical Response to Orographic Gravity Wave Drag Hotspots-A Zonal Mean Perspective, Geophysical Research Letters, 48, 1–11, https://doi.org/10.1029/2021GL093305, 2021.

Samtleben, N., Kuchař, A., Šácha, P., Pišoft, P., and Jacobi, C.: Mutual Interference of Local Gravity Wave Forcings in the Stratosphere, Atmosphere, 11, https://doi.org/10.3390/atmos11111249, 2020.

Scinocca, J. and McFarlane, N.: The parametrization of drag induced by stratified flow over anisotropic orography, Quarterly Journal of the Royal Meteorological Society, 126, 2353–2393, https://doi.org/10.1002/qj.49712656802, 2000.

Scinocca, J., McFarlane, N., Lazare, M., Li, J., and Plummer, D.: The CCCma third generation AGCM and its extension into the middle atmosphere, Atmospheric Chemistry and Physics, 8, 7055–7074, https://doi.org/10.5194/acp-8-7055-2008, 2008.

Scinocca, J. F.: An accurate spectral nonorographic gravity wave drag parameterization for general circulation models, Journal of the Atmospheric Sciences, 60, 667–682, 2003.

Sigmond, M., Anstey, J., Arora, V., Digby, R., Gillett, N., Kharin, V., Merryfield, W., Reader, C., Scinocca, J., Swart, N., et al.: Improvements in the Canadian Earth system model (CanESM) through systematic model analysis: CanESM5. 0 and CanESM5. 1, Geoscientific Model Development, 16, 6553–6591, https://doi.org/10.5194/gmd-16-6553-2023, 2023.

Simmons, A., Soci, C., Nicolas, J., Bell, B., Berrisford, P., Dragani, R., Flemming, J., Haimberger, L., Healy, S., Hersbach, H., et al.: ERA5.1: Rerun of the Fifth generation of ECMWF atmospheric reanalyses of the global climate (2000-2006 only), Copernicus Climate Change Service (C3S) Data Store (CDS), data distribution by the German Climate Computing Center (DKRZ), 2020.